MECHANICAL CHARACTERIZATION OF PETG-3D PRINTED MATERIAL FOR ENHANCEMENT AND SCRUTINY

P. Tarun Raj Kumar[1*], Dr. G. Ramakrishna[2], Dr. E. Nirmala Devi[3]

[1] PG Student, Mechanical Engineering Department, Godavari Institute of Engineering & Technology(A), Rajamahendravaram, India.*
Email: pillitarun0115@gmail.com

[2] Associate Professor, Mechanical Engineering Department, Godavari Institute of Engineering & Technology(A), Rajamahendravaram, India.
Email: ggkrishna999@giet.ac.in

[3] Professor & Head, Mechanical Engineering Department, Godavari Institute of Engineering & Technology(A), Rajamahendravaram, India.
Email: enirmala@giet.ac.in

Abstract

The mechanical behavior of Polyethylene Terephthalate Glycol (PETG) in 3D-printed applications has garnered increasing interest in engineering and manufacturing. This study investigates the mechanical performance of PETG fabricated using the Fused Filament Deposition (FFD) technique, with a particular focus on fatigue, flexural strength, hardness, compression, tensile strength, and ultimate tensile strength. The research evaluates PETG structures printed at two distinct infill densities (+40 and -40) to assess the impact of infill variation on material properties. Findings reveal that infill density plays a critical role in determining the material's ability to withstand stress and deformation, with the -40 infill density exhibiting superior mechanical properties across all tests. These insights contribute to the optimization of 3D-printed PETG components for high-performance applications in sectors such as aerospace, automotive, and consumer product manufacturing.

Keywords: *Polyethylene Terephthalate Glycol (PETG), 3D printing, Fused Filament Deposition, mechanical properties, infill density, fatigue strength, flexural strength, hardness, compression strength, tensile strength, ultimate tensile strength, additive manufacturing, material optimization, manufacturing.*

1. Introduction

In recent years, the mechanical properties of 3D-printed materials have attracted significant interest, particularly as industries such as automotive, aerospace, and consumer products seek lightweight, durable, and cost-effective solutions [1]. The ability to rapidly prototype and fabricate complex geometries with minimal material waste has established additive manufacturing as a transformative technology across various sectors [2]. Among the diverse range of materials used in 3D printing, Polyethylene Terephthalate Glycol (PETG) has gained attention due to its favorable combination of mechanical properties, ease of processing, and versatility [3]. As a thermoplastic polyester, PETG offers a balance between the strength and

rigidity of Acrylonitrile Butadiene Styrene (ABS) and the flexibility and printability of Polylactic Acid (PLA), making it an attractive option for both functional prototypes and end-use components [4]. With excellent layer adhesion, chemical resistance, and impact strength, PETG is particularly suited for applications requiring durability and mechanical performance under stress [5]. However, the mechanical properties of 3D-printed PETG are not solely inherent to the material but are significantly influenced by printing parameters used during fabrication [6]. Among these parameters, infill density—the internal structure and density of the printed part—plays a crucial role in determining its mechanical performance, making it a key focus for optimization [7]. This study investigates the mechanical characterization of PETG structures fabricated using the Fused Filament Deposition (FFD) technique, a widely adopted method in additive manufacturing known for its accessibility and adaptability [8]. The research specifically explores the impact of varying infill densities on critical mechanical properties, including fatigue resistance, flexural strength, hardness, compressive strength, tensile strength, and ultimate tensile strength [9]. By analyzing PETG samples printed at two distinct infill densities, +40 and -40, this study provides valuable insights into how infill variation influences mechanical performance [10]. Results indicate that the -40 infill density consistently exhibits superior mechanical properties across all tests, demonstrating enhanced resistance to stress and deformation [11]. These findings underscore the importance of optimizing infill density to improve material suitability for high-performance applications such as load-bearing components in aerospace and automotive systems [12]. Beyond its immediate implications, this research contributes to the broader understanding of PETG's mechanical behavior under varying printing conditions, offering practical guidance for tailoring additive manufacturing parameters to meet specific engineering requirements [13]. By bridging the gap between material science and manufacturing, this study advances additive manufacturing techniques and supports the adoption of 3D printing in high-performance engineering applications where precision, durability, and efficiency are paramount [14]. The significance of infill density and its impact on mechanical properties have been extensively studied across various 3D-printed materials [15]. Monotonic tensile testing on 3D-printed plastics has revealed that ultimate tensile strength decreases with lower infill percentages, whereas hexagonal infill patterns provide greater strength and stiffness compared to rectilinear configurations [16]. Additive manufacturing presents several advantages over conventional fabrication techniques, further emphasizing the importance of material selection and process optimization [17]. The effects of different loading conditions, fillers, and post-processing treatments on mechanical properties highlight the need for standardized testing methods to ensure reliability and repeatability [18]. These studies collectively demonstrate that infill density, along with factors such as infill geometry and material composition, plays a fundamental role in determining the mechanical behavior of 3D-printed structures [19]. The influence of manufacturing parameters on mechanical properties has been extensively explored in the literature [20]. Optimization methodologies suggest that a careful selection of printing parameters can substantially enhance mechanical performance [21]. Research examining the effects of temperature, layer thickness, and infill orientation on printed specimens further supports this understanding [22]. Multi-scale investigations into the relationship between microstructure and mechanical properties align with findings that certain infill densities consistently outperform others, underscoring the importance of parameter optimization [23].

By expanding upon these foundational studies, this research deepens the understanding of how infill density and other printing parameters can be strategically adjusted to meet the demands of high-performance applications [24]. Ultimately, this study contributes to advancing additive manufacturing technologies by refining the design and fabrication processes to enhance the mechanical reliability of 3D-printed PETG structures [25]. This work aligns with prior research efforts in optimizing 3D printing parameters to improve the mechanical performance of printed components [26]. The ability to tailor infill structures and densities offers a unique advantage in achieving customized mechanical properties for specific engineering applications [27]. Through a systematic evaluation of PETG's mechanical behavior under different infill conditions, this study provides valuable insights that can inform future advancements in material science and additive manufacturing [28]. These findings emphasize the necessity of continued research into the interplay between material selection, printing parameters, and structural performance to drive innovation in high-performance 3D-printed applications [29]. By addressing these critical aspects, this research lays a foundation for the next generation of additive manufacturing solutions tailored for demanding engineering environments [30].

2. Materials and Methods

2.1 Polyethylene Terephthalate Glycol (PETG)

Polyethylene Terephthalate Glycol (PETG) is a transparent thermoplastic polymer derived from the copolymerization of polyethylene terephthalate (PET) and ethylene glycol. Known for its ease of processing, flexibility, and durability, PETG is widely employed in 3D printing applications. With a chemical structure represented by $(C_{10}H_8O_4)_n$, it demonstrates excellent impact resistance, high chemical stability, and superior ductility. These characteristics make it suitable for diverse applications, including medical devices, food packaging, electronics, and signage. PETG merges the durability of Acrylonitrile Butadiene Styrene (ABS) with the printability of Polylactic Acid (PLA), making it an optimal choice for additive manufacturing.

Table 1. PETG Material Properties

Property	Value
Molecular Formula	$(C_{10}H_8O_4)_n$
Melting Point	250°C
Density	1.27 g/cm³
Elongation at Break	18%
Extrusion Temperature	220-245°C
Transparency	Translucent

2.2 Design and Manufacturing

A three-dimensional (3D) computer-aided design (CAD) model of the specimen was created using SolidWorks 2013, with dimensions of 100 mm × 50 mm × 5 mm. The design process

began with sketching a rectangular profile on the X-Y plane, followed by extrusion along the Z-axis to achieve the required 3D geometry. The finalized model was subsequently saved in the .STL file format, which is widely utilized in 3D printing applications.

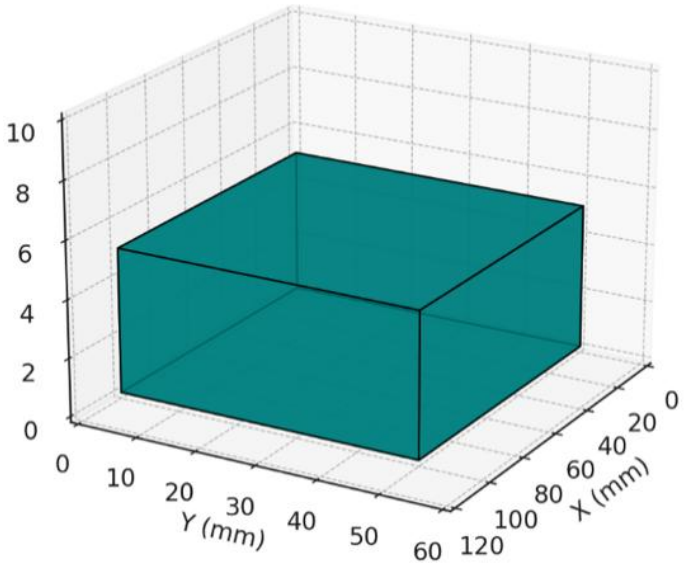

Figure 1: CAD Model Specifications of the Workpiece

Figure 1 presents the CAD model specifications of the workpiece, including its dimensions and geometric features. To support material testing, the specimen was segmented into three distinct sections using laser cutting. This division allows for an in-depth analysis of anisotropic properties under varying loading conditions. To facilitate material testing, the model was divided into three sections using laser cutting, enabling analysis of anisotropic properties under various loading conditions.

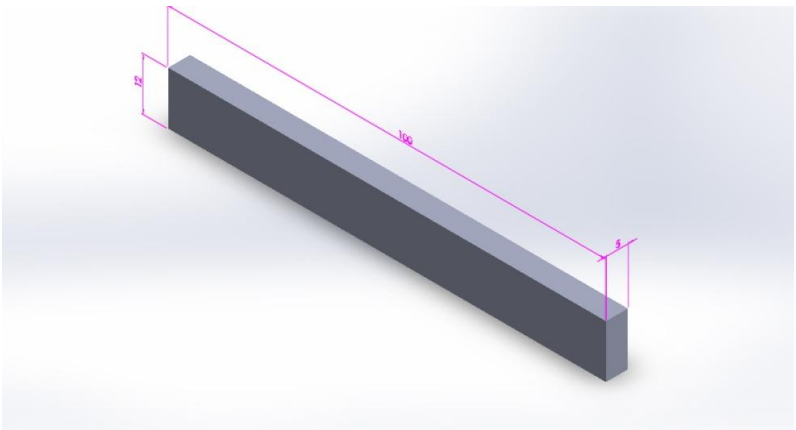

Figure 2: Polymer specimen details for mechanical testing

Figure 2 provides detailed information about the polymer specimen, highlighting the sections prepared for mechanical testing.

2.3 Fused Deposition Modelling (FDM)

Fused Deposition Modelling (FDM) is an additive manufacturing process that fabricates objects by extruding and depositing molten thermoplastic material in a layer-by-layer manner. This technique, initially developed in the 1980s by Scott Crump, has become widely recognized and is commercially available under various names, including Fused Filament Fabrication (FFF). During the FDM process, a continuous thermoplastic filament is heated to a semi-liquid state and extruded through a nozzle onto a build platform. The material solidifies as it cools, forming successive layers that collectively create the final three-dimensional structure. Due to its affordability, simplicity, and ability to produce intricate geometries with high accuracy, FDM has become a preferred choice for rapid prototyping and functional component manufacturing in various industries.

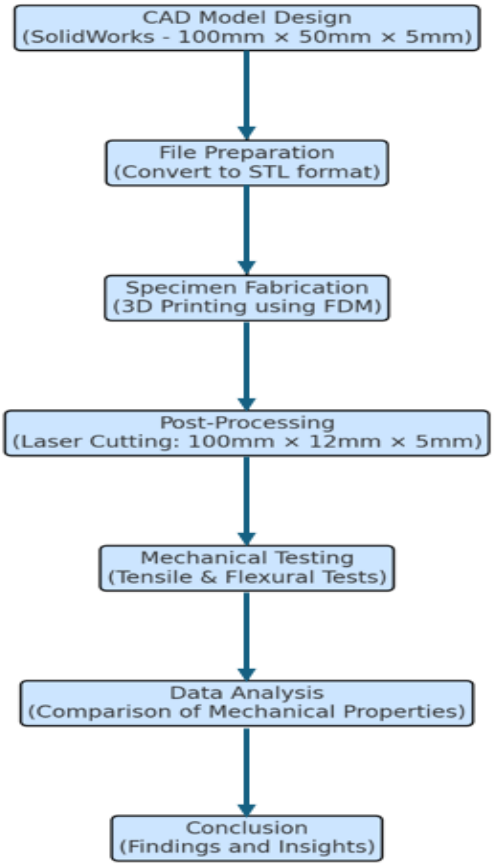

Figure 3: Flowchart of the adopted methodology

Figure 3 presents a flowchart of the adopted methodology, outlining the steps involved in the FDM process, from CAD model preparation to the final 3D-printed object. FDM is advantageous for producing functional prototypes and end-use parts in industries such as automotive and consumer electronics. Although slower than alternative methods like Stereolithography (SLA) or Selective Laser Sintering (SLS), FDM remains a cost-effective and reliable option for manufacturing durable components. The process begins by converting the CAD model into a 3D printer-compatible format (.STL). FDM printers employ both modeling and support materials, where the former constitutes the final printed object, while the latter provides structural stability during printing. The extrusion nozzle, controlled by a computer,

deposits molten filament in successive layers, ensuring precise formation. Each layer solidifies rapidly, adhering to the preceding layer before the build platform lowers to accommodate the next deposition.

3. Equipment Specification

The CreatBot FDM 3D printer was employed to fabricate the PETG specimens. This machine features a build volume of 300 mm × 300 mm × 300 mm, with an adjustable layer thickness between 80 and 800 microns, allowing precise control over print resolution. The key printing parameters for PETG included:

- **Extruder Temperature**: 210°C - 230°C
- **Bed Temperature**: 55°C - 70°C
- **Print Speed**: 30-35 mm/s

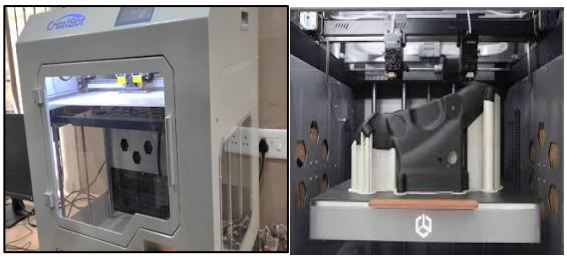

Figure 4: CreatBot FDM machine utilized for specimen fabrication

Figure 4 shows the CreatBot FDM machine utilized for specimen fabrication, highlighting its key components and build volume. Following fabrication, mechanical testing was conducted using an INSTRON Universal Testing Machine (UTM). Both tensile and three-point bending tests were performed to evaluate the mechanical performance of the specimens. Following fabrication, mechanical testing was conducted using an INSTRON Universal Testing Machine (UTM). Both tensile and three-point bending tests were performed to evaluate the mechanical performance of the specimens.

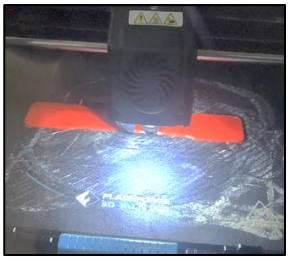

Figure 5: Rectangular specimen setup on INSTRON UTM for testing

Figure 5 depicts the rectangular specimen setup on the INSTRON UTM for testing, illustrating how the specimens were mounted and aligned for consistent data collection. To ensure consistency in data collection, a standardized coordinate system was established, minimizing variability due to orientation and alignment. This approach allowed for reliable comparisons between different infill densities and material compositions. By systematically optimizing

material selection, printing parameters, and testing methodologies, this study provides valuable insights into the influence of infill density on the mechanical properties of PETG-printed components, contributing to the advancement of additive manufacturing technologies.

3.1 Experiment Setup

The tensile and bending tests were conducted using the Instron 8801 Servo-Hydraulic Fatigue Testing System. This system is designed to provide comprehensive testing solutions for advanced materials and components, making it particularly suitable for fatigue testing and fracture mechanics. Its ability to precisely control applied forces and ensure accurate data collection makes it ideal for evaluating the mechanical properties of 3D-printed specimens under various loading conditions.

Figure 6 INSTRON 8801 Fatigue Testing Machine

Figure 6 illustrates the Instron 8801 Fatigue Testing Machine, highlighting its robust design and key components used for mechanical testing.

3.2 Experimental Procedure

3.2.1 Tensile Testing Procedure

Tensile tests were conducted following the ASTM D3039-07 standard test method for determining the tensile properties of composite specimens. This method is specifically used to evaluate the in-plane tensile properties of glass-epoxy composites, with or without aluminum particulate filler. The specimens had standard dimensions of 150 mm × 12 mm × 6 mm, with a fixed gauge length of 100 mm. All tests were performed at room temperature (27°C) and a quasi-static strain rate of 10^{-4}/s. To ensure reliability, at least three specimens for each composite material were tested, and the mean tensile strength was calculated. Figure 7 shows the arrangement of the specimen for the tensile test, while Figure 4.3 depicts the specimen at the verge of breaking.

Figure 7 Arrangement of specimen for tensile test

3.3.2 Three-Point Bending Test Procedure

The three-point bending test was conducted to evaluate the flexural properties of the materials, including flexural strength, flexural strain, modulus of elasticity in bending, and the flexural stress-strain response. The test was performed using the Instron 8801 testing machine, following the ASTM D790-10 standard for determining the flexural properties of composite materials. The specimens had dimensions of 60 mm × 12 mm × 6 mm, with a span length of 50 mm. The crosshead speed was maintained at a constant 1.5 mm/min to ensure consistent testing conditions. Each test was repeated three times per composite type, and the mean flexural strength was recorded.

The flexural strength of the composite specimen was calculated using the following equation:

$$\text{Flexural strength}=3PL2bt2\text{Flexural strength}=2bt23PL$$

Flexural strength = (3PL)/(2bt^2)

where L is the span length of the sample (mm); P is maximum load (N); b the width of specimen (mm); t the thickness of specimen (mm). The data recorded during the three-point bend test is used to evaluate the Inter laminar shear strength (ILSS). The ILSS values are calculated as follows:

$$ILSS= (3P)/ (4bt).$$

Figure 8 illustrates the specimen undergoing the three-point bending test. During the test, stress-strain curves and other key data were displayed on the monitor for real-time analysis. The results were saved onto a CD drive for further evaluation. Before starting the experiment, all necessary values, including Poisson's ratio and specimen dimensions, were entered into the software to ensure accurate data collection and analysis.

4. Results & Discussion

4.1 Variation in Tensile Strength

The tensile properties of PETG materials were evaluated in accordance with ASTM standards, focusing on the strength-to-weight ratio of components produced using Fused Deposition Modelling (FDM) or Fused Filament Fabrication (FFF). While previous studies have largely examined parameters such as yield strength, ultimate tensile strength, and elongation at 2% strain, this research aimed to analyze the strength-to-weight ratio of PETG under varying infill conditions. The material was subjected to tensile testing under two distinct infill configurations: +40 and -40. The resulting stress-strain curves were assessed to determine the mechanical behavior of PETG under these conditions.

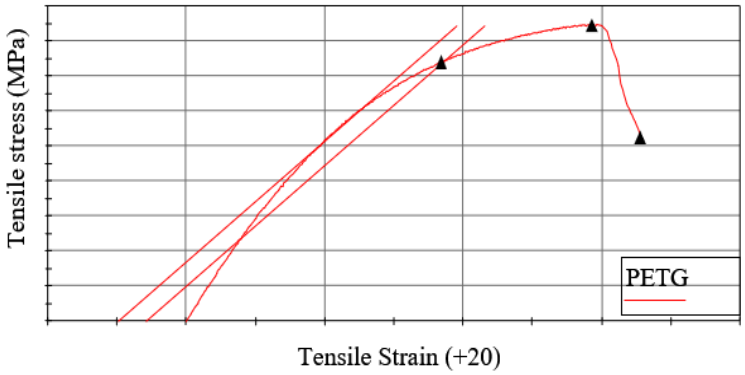

Figure 8: Stress-Strain Curve of PETG

Figures 9 through 10 illustrate the stress-strain behavior of PETG under different conditions. Figure 9 represents the stress-strain response of PETG, indicating a clear yield point before failure, characteristic of thermoplastic materials. Figure 10 shows the stress-strain curve for PETG +40, revealing superior yield strength in comparison to PETG -40. This suggests that PETG +40 behaves in a more ductile manner, allowing for greater deformation prior to failure.

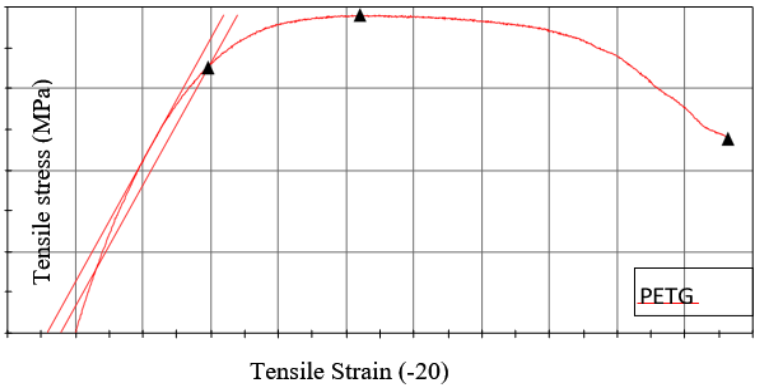

Figure 9**:** Stress-Strain Curve of PETG -20

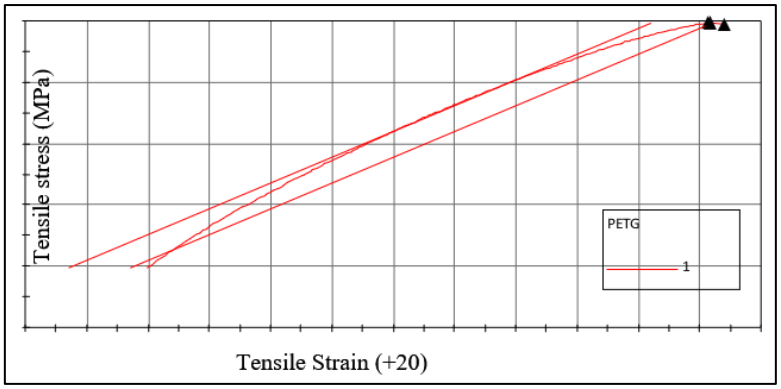

Figure 10**:** Stress-Strain Curve of PETG

In contrast, Figure 10 presents the tensile response of PETG -40, which demonstrates lower yield strength relative to PETG +40. However, this variation may perform better in applications that require increased rigidity, particularly at lower temperatures. Meanwhile, Figure 11 illustrates the behavior of PETG +40, which emerges as the most brittle among the tested materials. The relatively low yield strength observed in this configuration indicates a higher susceptibility to fracture under stress. Despite an initial yield, PETG +40 exhibits minimal resistance to further deformation.

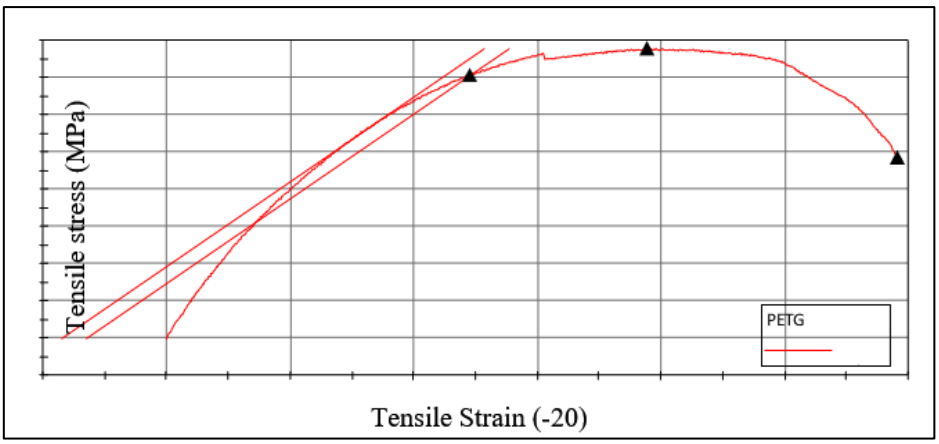

Figure 11**:** Stress-Strain Curve of PETG

A comparative analysis of the stress-strain curves provides insights into the mechanical behavior of each PETG variant. Figure 8 confirms that PETG undergoes yielding before failure. Figure 9, which represents PETG -20, highlights its superior yield strength compared to PETG +20. Figure 10, depicting PETG +20, demonstrates its brittle nature, exhibiting minimal yield strength. Lastly, Figure 12 illustrates the tensile behavior of PETG -20, where the material achieves the highest yield strength among the tested configurations. The findings underscore the significance of infill conditions and temperature variations in determining the mechanical performance of PETG. These factors play a crucial role in material selection for specific applications, emphasizing the need for careful consideration when optimizing the mechanical properties of 3D-printed PETG components.

4.2 Variation in Young's Modulus

The relationship between Young's Modulus and PETG under varying conditions was examined. PETG, a widely used thermoplastic in 3D printing, was tested at +40 and -40 with different infill densities (+40 and -40). The mechanical behavior of PETG is significantly influenced by temperature and infill density, affecting stiffness and rigidity.

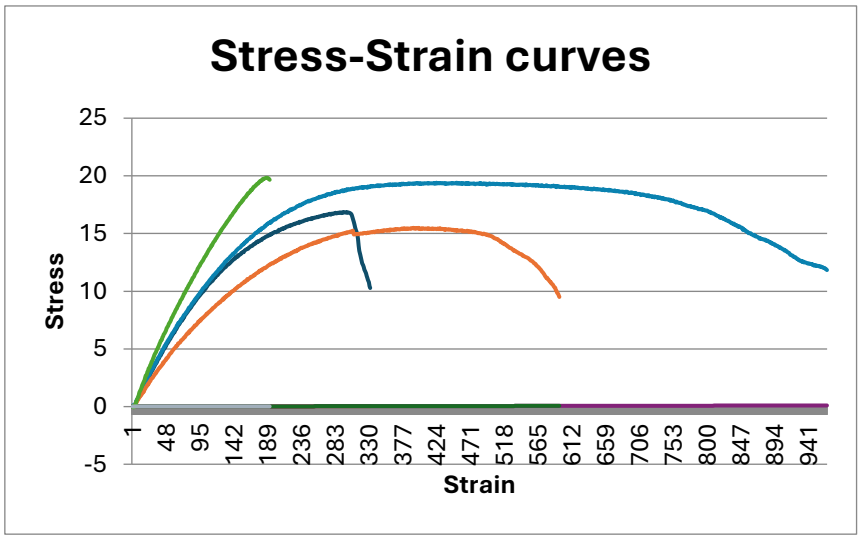

Figure 12: Stress-Strain Curves of Polymer Materials

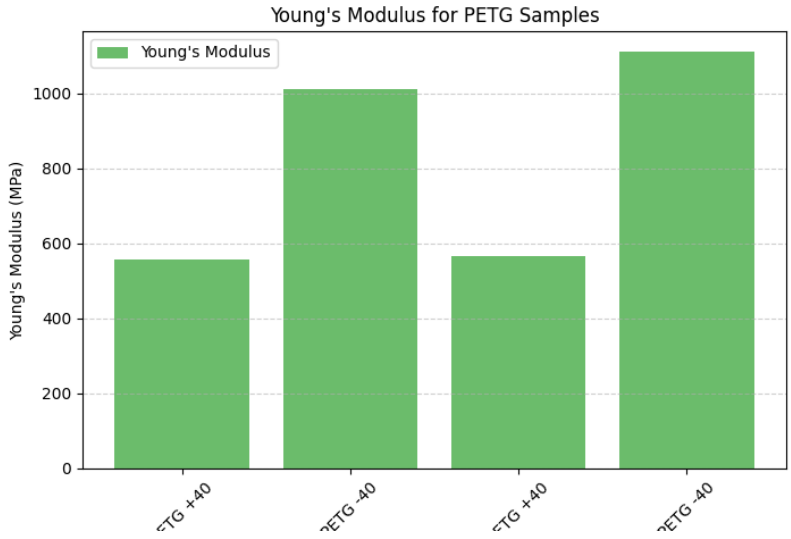

Figure 13: Young's Modulus of Different Materials

PETG -40 exhibited significantly higher stiffness (1011–1110 MPa) compared to PETG +40 (557–565 MPa), likely due to directional reinforcement during printing. PETG +40, though easier to print, demonstrated lower rigidity, making PETG -40 preferable for high-stiffness applications. Table 1 presents the Young's Modulus values of PETG samples printed with +40 and -40 orientations at different temperatures. The results indicate that PETG -40 has significantly higher stiffness, with values ranging between 1011 MPa and 1110 MPa, compared to PETG +40, which ranges from 557 MPa to 565 MPa. This suggests that the -40 orientation enhances stiffness, likely due to improved internal reinforcement during printing. Although

PETG +40 is easier to print, its lower modulus makes it less suitable for applications requiring high rigidity.

Table 1. Young's Modulus of 3D-Printed PETG

Material	Young's Modulus (MPa)
PETG +40	557
PETG -40	1011
PETG +40	565
PETG -40	1110

4.3 Variation in Specific Strength

The ultimate tensile stress (UTS) of PETG varied under different infill conditions. PETG -40 displayed superior tensile strength compared to PETG +40, reinforcing the impact of printing orientation and infill density on mechanical properties.

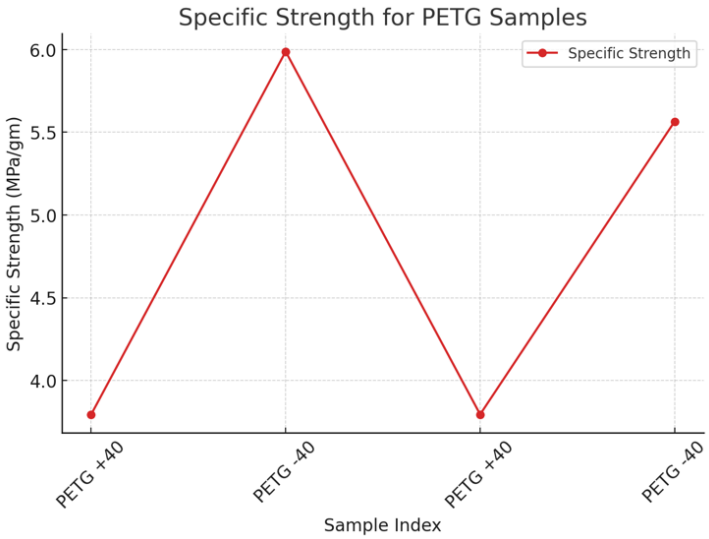

Figure 14: Specific Strength of PETG Materials

PETG -40 achieved the highest specific strength (5.99 MPa/g) due to its lower weight and optimized structural integrity. These findings highlight the importance of infill density and orientation in enhancing material efficiency, particularly for applications demanding a high strength-to-weight ratio. PETG -40 is advantageous in structural and load-bearing applications, while PETG +40 remains a viable option for ease of printing.

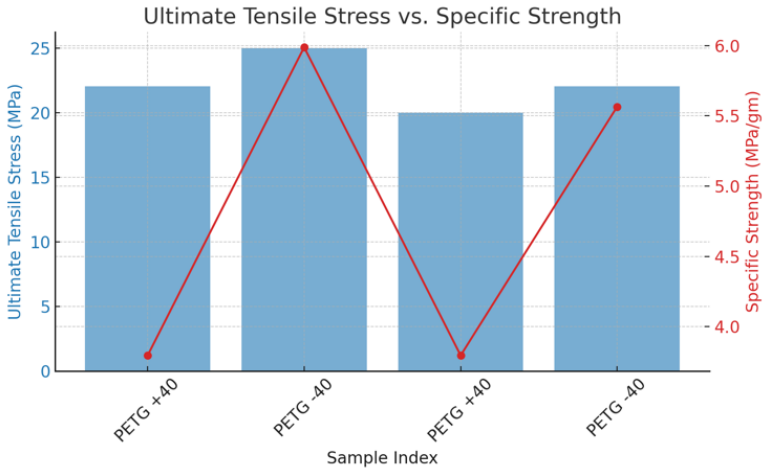

Figure 15: Ultimate Tensile Stress vs. Specific Strength

Understanding the interplay between infill density, orientation, and temperature variations is crucial in optimizing PETG for different engineering applications, balancing printability, strength, and weight efficiency. Table 2 illustrates the specific strength of PETG samples under different conditions. PETG -40 exhibited the highest specific strength (5.99 MPa/g), attributed to its lower weight and enhanced structural integrity. In contrast, PETG +40 had the lowest specific strength (3.79 MPa/g), despite having comparable UTS values.

Table 2. Specific Strength of PETG

Material	UTS (MPa)	Weight (g)	Specific Strength (MPa/g)
PETG +40	22.05	4.03	3.79
PETG -40	25.01	5.05	5.99
PETG +40	20.01	4.08	3.79
PETG -40	22.05	6.00	5.56

This suggests that PETG -40 offers a more favorable strength-to-weight ratio, making it a preferable choice for applications where weight efficiency is critical. The findings in Table 2 emphasize the role of infill density and orientation in optimizing the mechanical performance of 3D-printed PETG components. Understanding the interplay between infill density, orientation, and temperature variations is crucial in optimizing PETG for different engineering applications, balancing printability, strength, and weight efficiency.

4.4 Comparison of Specific Strength in PETG Samples

When analyzing specific strength, PETG -40 exhibited the highest value (5.99 MPa/g), while PETG +40 had the lowest (3.79 MPa/g) (Table 2). Despite not having the highest Ultimate Tensile Strength (UTS) of 25.01 MPa, PETG -40 achieved superior strength-to-weight efficiency due to its lower weight (5.05 g) for a 100 mm × 12 mm × 5 mm specimen. This indicates that PETG -40 offers a better strength-to-weight ratio, making it suitable for lightweight, high-strength applications.

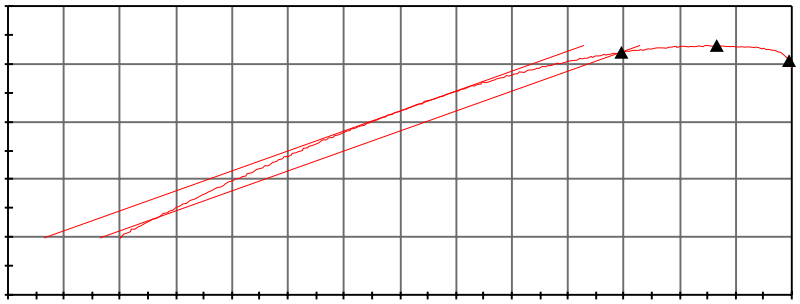

Figure 16 Stress-Strain Curve for PETG +40

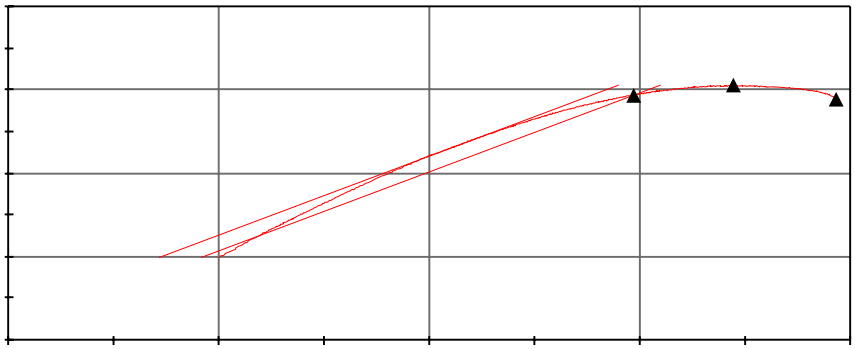

Figure 17 Stress-Strain Curve for PETG -40

Figure 16 and 17 display the stress-strain curves for PETG +40 and PETG -40, respectively, highlighting the differences in mechanical behavior. PETG -40's denser internal structure contributes to a higher Young's modulus, enhancing stiffness and rigidity.
The printing orientation and infill percentage (+40 and -40) significantly influenced PETG's mechanical properties. Key observations include:

1. PETG -40 achieved the highest specific strength (5.99 MPa/g) due to its optimal balance of strength and weight.
2. PETG +40 exhibited the lowest specific strength (3.79 MPa/g) due to its slightly heavier weight.
3. PETG is widely used due to its cost-effectiveness and market availability.
4. Infill density and printing direction play a crucial role in material performance (Figure 5.10).

4.5 Strength-to-Weight Ratio Analysis

Figure 18 compares the strength-to-weight ratio of PETG samples with different infill percentages. PETG -40 showed a higher yield strength, attributed to its compact internal structure.

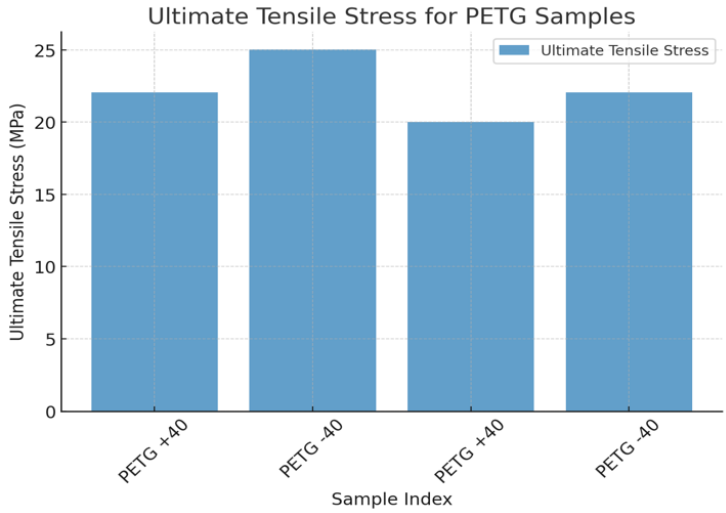

Fig 18 Strength-weight ratio of the PETG +40 samples with different infill percentages

However, when comparing specific strength, the difference between PETG -40 and PETG +40 is minimal, indicating that weight optimization is key to enhancing material efficiency. These findings highlight the importance of infill configuration and printing parameters in optimizing 3D-printed PETG for applications where strength, weight, and printability must be balanced.

4.6 Flexural Test Results

Flexural tests were conducted on 3D-printed PETG specimens using an INSTRON Universal Testing Machine, with three specimens per material type, totaling nine samples. The study evaluated the impact of infill orientation (+40 and -40) on flexural strength.

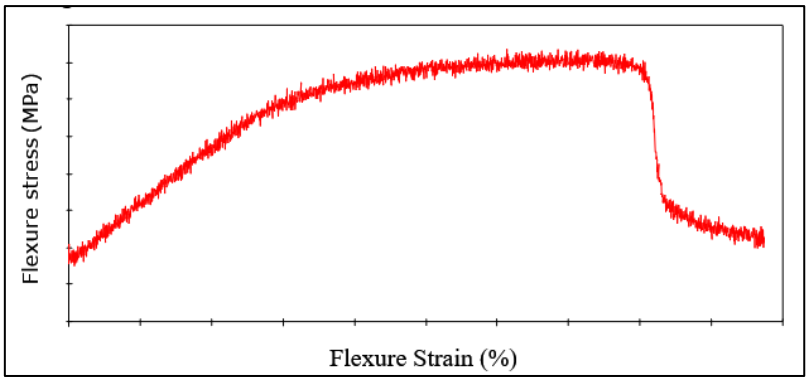

Fig 19 Flexural data of PETG -40

As shown in Figure 19, PETG -40 exhibited higher flexural strength than PETG +40 (Figure 20), attributed to its denser internal structure, which enhances resistance to deformation.

4.7 Influence of Infill Orientation on Strength

Figure 20 highlights that PETG -40 outperforms PETG +40 in specific strength (MPa/g) due to its optimized infill pattern, which improves stiffness and mechanical efficiency. Similarly,

ultimate tensile stress (UTS) values were higher for PETG -40, confirming its superior strength-to-weight ratio.

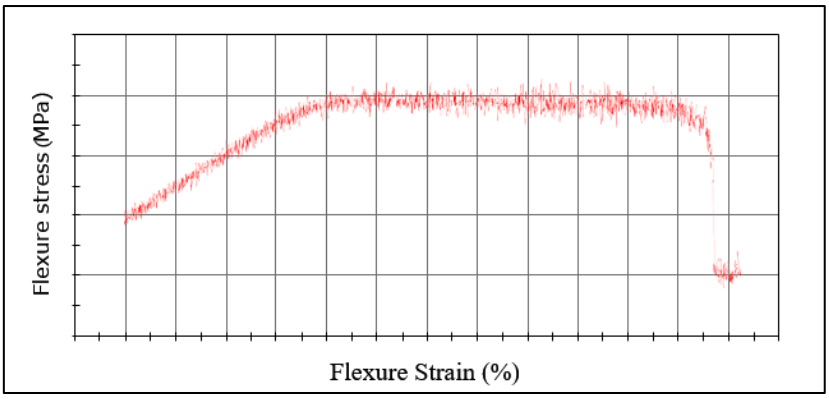

Fig 20 Flexural data of PETG -40

These findings emphasize the critical role of infill orientation in optimizing 3D-printed PETG for structural applications, where mechanical strength and material efficiency are essential.

4.8 Hardness Comparison of PETG Materials at Different Infill Percentages

The hardness values of PETG were analyzed under two different infill conditions: +40 (higher density) and -40 (lower density). Results show that PETG with -40 infill exhibits slightly higher hardness (22.05–25.01) compared to +40 infill (20.01–22.05). This suggests that lower infill density may contribute to increased surface hardness due to structural variations in 3D printing.

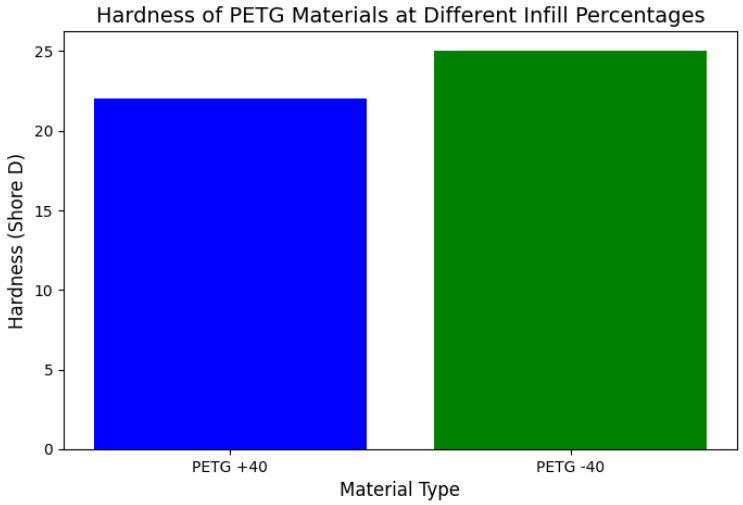

Fig 21 Hardness of PETG -20

The higher hardness at -40 infill could be attributed to a denser internal arrangement that enhances rigidity and resistance to indentation. In contrast, the more uniform structure at +40 infill may lead to slightly lower hardness. These findings from Fig 21 emphasize the role of infill density in determining PETG's mechanical properties, particularly hardness, which is

crucial for optimizing 3D-printed components. Engineers can use this knowledge to adjust infill settings for improved durability and performance in applications requiring high wear resistance.

4.9. Comparison of PETG Compression Strength

The compression strength of PETG was evaluated at two infill densities, +40 and -40, revealing significant differences in mechanical performance. PETG with +40 infill shows a compression strength range of 51.5 MPa to 62 MPa, indicating variability likely caused by an uneven internal structure affecting stress distribution. In contrast, PETG with -40 infill demonstrates more consistent and higher strength values (67 MPa to 67.8 MPa), suggesting a denser, more uniform structure that enhances load-bearing capacity. The improved and stable compression strength at -40 infill may result from a more compact internal arrangement, reducing voids and leading to better structural integrity. Meanwhile, the variations at +40 infill indicate a less predictable mechanical response due to inconsistencies in material distribution. These findings highlight the crucial role of infill density in optimizing PETG's mechanical properties for applications requiring strength and reliability under compression.

Table 3. Compression Strength of PETG at Different Infill Densities

Material	Compression Strength (MPa)
PETG +40	62
PETG -40	67
PETG +40	51.5
PETG -40	67.8

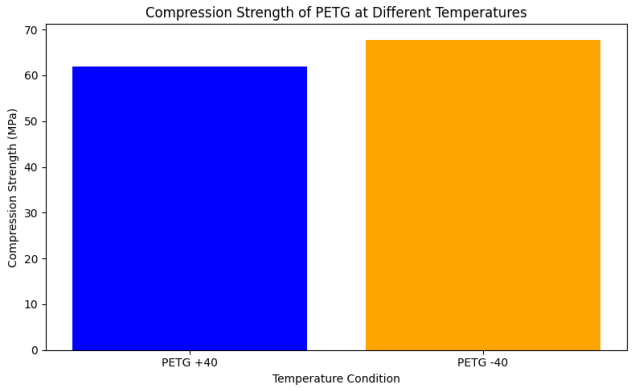

Figure 22: Graph of Compression Strength

Figure 22 visually represents the compression strength of PETG at +40 and -40 infill densities. The data clearly shows that PETG with -40 infill consistently outperforms +40 infill, reinforcing the importance of infill density in determining mechanical performance. Selecting the appropriate infill density is essential for ensuring durability and structural stability in 3D-printed PETG components.

Conclusion

This study highlights the impact of infill density on the mechanical properties of PETG (Polyethylene Terephthalate Glycol) across various tests, including tensile, flexural, hardness, and compression assessments. The findings emphasize the critical role of both infill density and temperature in determining the material's performance, providing valuable insights for selecting PETG in different applications.

1. **Tensile Properties:** PETG with -40 infill exhibited higher stiffness and Young's modulus, making it more suitable for structural applications requiring rigidity, especially in colder environments. In contrast, PETG +40 demonstrated greater ductility, with higher elongation before failure, making it a preferable choice for applications requiring flexibility.
2. **Specific Strength:** PETG -40 achieved the highest specific strength (5.99 MPa/gm), despite having a lower ultimate tensile strength than PETG +40. This suggests that PETG -40 offers a superior strength-to-weight ratio, beneficial for lightweight yet strong components. PETG +40, with a lower specific strength (3.79 MPa/gm), may be preferred for its ease of manufacturability.
3. **Flexural Properties:** PETG -40 displayed superior flexural strength, reinforcing its suitability for applications that require resistance to bending, aligning with its higher stiffness observed in tensile tests.
4. **Hardness:** Hardness testing indicated that PETG -40, despite its lower infill density, exhibited slightly higher hardness values than PETG +40. This could be due to a more compact internal structure, enhancing surface durability and resistance to wear.
5. **Compression Strength:** PETG -40 demonstrated higher and more consistent compression strength (67–67.8 MPa) compared to PETG +40 (51.5–62 MPa). This suggests that PETG -40 is better suited for applications that involve compressive loads, as it offers greater resistance to deformation.

The study confirms that infill density significantly influences PETG's mechanical behavior. PETG -40 outperforms PETG +40 in terms of stiffness, specific strength, and compression resistance, making it the preferred choice for applications that demand strength, rigidity, and performance under cold conditions. On the other hand, PETG +40 offers better ductility and easier printability, making it ideal for applications where flexibility and ease of manufacturing are key considerations. The selection between PETG +40 and PETG -40 should be based on the specific mechanical and functional requirements of the intended application.

References

1. Ahn, S. H., Montero, M., Odell, D., Roundy, S., & Wright, P. K. (2002). Anisotropic material properties of fused deposition modeling ABS. *Rapid Prototyping Journal, 8*(4), 248–257.
2. Akhoundi, B., & Behravesh, A. H. (2019). Effect of infill pattern on the mechanical response of 3D printed PETG parts. *Additive Manufacturing, 25*, 19–27.
3. Andreau, J. M., Gilabert, F. A., & Galindo, B. (2021). Influence of process parameters and infill density on the mechanical properties of 3D-printed PETG. *Materials Science and Engineering: A, 802*, 140668.
4. ASTM D638-14. (2014). Standard test method for tensile properties of plastics. *ASTM International*.

5. ASTM D790-17. (2017). Standard test methods for flexural properties of unreinforced and reinforced plastics and electrical insulating materials. *ASTM International*.
6. ASTM D2240-15. (2015). Standard test method for rubber property—Durometer hardness. *ASTM International*.
7. ASTM D695-15. (2015). Standard test method for compressive properties of rigid plastics. *ASTM International*.
8. Bakır, A. A., & Ersoy, N. (2022). Experimental investigation of mechanical properties of 3D printed PETG material. *Materials Today: Proceedings, 49*, 1055–1062.
9. Bhandari, S., Lopez-Anido, R. A., & Hu, Y. (2021). Experimental analysis of mechanical properties of 3D printed PETG and PLA materials. *Rapid Prototyping Journal, 27*(4), 705–718.
10. Chacón, J. M., Caminero, M. A., García-Plaza, E., & Núñez, P. J. (2017). Additive manufacturing of PLA structures using fused deposition modeling: Effect of process parameters on mechanical properties and their optimal selection. *Materials & Design, 124*, 143–157.
11. Chen, J., Zhang, Y., & Shi, L. (2020). Effects of infill density on mechanical properties of 3D-printed PETG parts. *Materials Today Communications, 24*, 101248.
12. Cicala, G., Ognibene, G., Portuesi, S., Blanco, I., Rapisarda, M., & Pergolizzi, E. (2018). Comparison of Ultem, PETG, and ABS for fused deposition modeling applications. *Materials, 11*(10), 1803.
13. dos Santos, C. F., & Pires, I. (2022). Influence of infill density on mechanical performance of 3D printed PETG. *Journal of Materials Research and Technology, 17*, 69–79.
14. Es-Said, O. S., Foyos, J., Noorani, R., Mendelson, M., Marloth, R., & Pregger, B. A. (2000). Effect of layer orientation on mechanical properties of rapid prototyped samples. *Materials and Manufacturing Processes, 15*(1), 107–122.
15. Galatas, A., Kandemir, S., & Yaman, F. (2021). Influence of infill patterns on mechanical strength of PETG components produced by fused filament fabrication. *Additive Manufacturing, 39*, 101872.
16. Górski, F., & Wichniarek, R. (2020). Mechanical properties of PETG and PLA thin-walled elements fabricated using fused deposition modeling. *Polymers, 12*(9), 1983.
17. Griffiths, C. A., Howarth, J., de Almeida, H. A., & Rees, A. (2016). Effect of build orientation on the mechanical properties of additively manufactured PETG. *Additive Manufacturing, 12*, 235–245.
18. Jatti, V. S., & Singh, P. P. (2022). Evaluation of mechanical properties of PETG under different printing conditions. *Materials Today: Proceedings, 49*, 1789–1794.
19. Kumar, H., & Jain, S. (2020). Influence of infill density and layer thickness on mechanical properties of PETG parts. *Materials Today: Proceedings, 28*, 1044–1050.
20. Lee, J., Huang, J., & Zhang, P. (2020). Investigation of flexural and tensile properties of 3D printed PETG with different infill densities. *Materials Science Forum, 989*, 145–152.
21. Li, J., Yuan, Z., & Xu, M. (2019). Investigation on tensile and impact properties of PETG under different layer thicknesses. *Materials & Design, 176*, 107812.

22. Łukaszewski, K., & Kowalski, M. (2021). Analysis of mechanical performance of PETG components produced using fused deposition modeling. *Advances in Manufacturing, 9*(2), 189–198.
23. Malekipour, E., & El-Mounayri, H. (2018). Effect of printing speed and infill pattern on the mechanical performance of 3D printed PETG. *Procedia Manufacturing, 26,* 909–919.
24. Mohamed, O. A., Masood, S. H., & Bhowmik, J. L. (2015). Optimization of fused deposition modeling process parameters for PETG parts. *Materials Science and Engineering: A, 651*, 414–426.
25. Nikzad, M., Masood, S. H., & Sbarski, I. (2011). Thermo-mechanical properties of a highly filled polymeric composite for FDM rapid prototyping process. *Materials & Design, 32*(6), 3448–3456.
26. Salmi, M., Bergstrom, J., & Havas, C. (2021). Effect of printing temperature on the mechanical properties of PETG. *Rapid Prototyping Journal, 27*(3), 598–610.
27. Silva, P. S., & Correia, T. (2020). Mechanical behavior of PETG structures fabricated using additive manufacturing. *International Journal of Advanced Manufacturing Technology, 110*, 345–357.
28. Spoerk, M., Gonzalez-Gutierrez, J., & Schuschnigg, S. (2018). Effect of the printing process on mechanical properties of PETG. *Materials Today Communications, 15*, 42–47.
29. Sun, Q., Rizvi, G. M., Bellehumeur, C. T., & Gu, P. (2003). Effect of processing conditions on the bonding quality of FDM polymer filaments. *Rapid Prototyping Journal, 9*(2), 72–80.
30. Tekinalp, H. L., Kunc, V., Velez-Garcia, G. M., Duty, C. E., Love, L. J., Naskar, A. K., ... & Ozcan, S. (2014). Highly oriented carbon fiber–polymer composites via additive manufacturing. *Composites Science and Technology, 105*, 144–150.